The Modular Nonoverlapping Grasp Workspaces and Dynamics for the Grippers using the Micro and Macro C-Manifold Design

Haydar Sahin

Department of the Mechatronics Engineering, Istanbul Gedik University, Istanbul, 34 987, Turkey

The toolbox for the gripper workspace analyses using Lie algebra is developed for shape variables ($\alpha_{1\text{-}4} - \theta_{1,2}$) of the skew revolute joints. The unique methodology for grippers comprises to enable the variety of manifold analyses for kinematics and dynamics using symbolic mathematics. The Controllable Instantaneous Screw Axes (C-ISA) are defined through the shape variables considering the twists of the skew revolute joints **se(3)**. The derivation and analyses of the kinematics and dynamics equations are made possible using the developed methodology with the defined constraints for gripper mechanisms. The Modular Gripper with Lie Algebra Toolbox (M-GLAT) is developed for the defined constraints of the angle between C-ISA 1 and C-ISA 2. The novelty subject of this article is the development of the M-GLAT method for derivation of the constraint based workspaces with the shape variables ($\alpha_{1\text{-}4} - \theta_{1,2}$) in the field of the spatial 2-RR gripper mechanisms. The gripper dynamics with constraint based workspaces of the skew revolute joints are developed for varied configurations of $\alpha_{1\text{-}4}$ with ICs of $\theta_{1,2}$. The modular rule-based workspaces are analyzed for the shape variables of the ($\alpha_{1\text{-}4} - \theta_{1,2}$) with the task spaces. This design produces dexterity with the modular grasp workspaces for the gripper fingers with skew revolute joints. One can select a combination of C-manifolds of ($\pi/20$, $\pi/40$, $\pi/80$) for the requirement of the nonoverlapping workspaces of the gripper finger designs as the grasp surfaces to control. The modular nonoverlapping workspace design with dynamics herein is based on the shape variables ($\alpha_{1\text{-}4} - \theta_{1,2}$) using skew revolute joint which produce the high dexterity for the grasping capability of the grippers. The modular micro and macro C-manifold designs obtained the constraint based workspace algorithms of the 2-RR gripper which is expandable into the higher modular revolute joints of the n-R for the grippers. The n-R modular expandable grippers are increasing the precision and power grasping capability.

Keywords: Lie algebra, Lie group theory, Shape variables of skew revolute, Spatial robot kinematics and dynamics, Task space

Introduction

The configuration-dependent modular design considers spatial controllable instantaneous screw axis (C-ISA) orientation as a manifold of 2-RR modular robot parameters for specified applications. The novel modular design concept herein is developed using the 2-RR common mechanisms for the grippers of the service and industrial robots.[1] The two classifications herein of the 2-RR modular grippers for robots are micro and macro configuration-dependent modular designs analyzed in-depth in this research article with kinematic results. Additionally, the challenging era of symbolic mathematics of modern robot dynamics is emerging to derive the Equation of Motion (EOM) using the integrated Lie group theory. The Lie group theory analyzed the robot dynamics and kinematics thoroughly.[2–6] The skew revolute joints for the serial robots[7,8] are applicable herein for the gripper mechanisms with the skew axis of the C-ISA.

Gripper poses for the precision or power grasp herein can be modified using the algorithms developed from the M-GLAT.

The skew axis is a part of the mechanism common in the wrist and gripper designs. The decoupling for the wrist design is studied experimentally without considering the coupled dynamics and the kinematic equations.[9–11] Wrist joints have skew revolute axes. Additionally, the research in ISA has been specifying the motion pattern of the mechanism for the skew axis of rotation.[12] The 2-screw system, examined in this article, of the 2-RR robots are classified into special groups for kinematics analysis and control.[13,14] The advantage of the revolute joint with the skew axis is its high maintainability with the developed models for multibody dynamics in the literature.[15] The modular workspaces herewith the dynamics for the modular grippers are developed beside the results of workspaces and dynamics in this research article.

A toolbox with various constraints definable is an asset for a modular gripper design. Thus, the workspace of the gripper herein was analyzed using

─────────────
*Author for Correspondence
E-mail: haydar.sahin@gedik.edu.tr

the constraints of the angle between two C-ISA with a developed toolbox. The angle between the C-ISA 1 and C-ISA 2 is a constraint for the workspace design pivotal to define the modular grasp capability of the gripper. Therefore, the angle between the C-ISA 1 and C-ISA 2 is chosen as a constraint for the micro and macro configurations of the gripper herein. Thus, the purpose of this research article is to develop a multi-functional tool wherein the constraint-based kinematics and dynamics equations can be derived for the skew revolute joints of the n-R gripper mechanism. One would need the skew revolute joint to grasp complex objects in hand with high dexterity. Thus, the determination of the workspace for grasping surface is required for skew revolute mechanisms considering dynamics. Modular Gripper with Lie Algebra Toolbox (M-GLAT) is developed within the defined constraints of the angle between C-ISA 1 and 2. Additionally, various constraints herewith were defined using the *M-GLAT* for n-R gripper mechanisms such as 3-R. The novel modular micro and macro gripper workspaces via shape variables of ($\alpha_{1-4} - \theta_{1,2}$) are defined using the *M-GLAT* developed herein.

The *configuration spaces* (*C-space*) for the skew revolute joint mechanisms are specified based on the requested task spaces for path planning. The algorithms developed are for the obstacle avoidance of the robots based on this path planning strategy. The defined *C-space* is a position vector concerning spatial coordinate q $\in$ Q_1 of SE (3).[5,16] The $\mathbb{R}^3$ term defines the position of the end effector, while the SO (3) defines the orientation of the *C-space*. The transformation matrix of g_{1j_2} acting as Q_1 is a group variable of the SE (3) matrix for the position and orientation.[5,16] The *C-space* maps are the unification of the requested *C-spaces* for motion planning of the obstacle avoidance.

The configuration defines all the possible positions of the mechanisms with skew revolute joints. The group variable of *g* in SE (3) can be modified in Lie algebra as $g^{-1}\dot{g}$ in SE (3) the velocity. S is the shape space containing the shape variables of the ($\alpha_{1-4} - \theta_{1,2}$). The configuration of the modular structure defines the ($Q_2 = G \times S$) for the serial robots.[17] The configuration of the robots is congruent with the matched shape variables *S* of the group variables *G*. The set cluster of the group variables with the shape variables of S can structure all the possible positions for the mechanism as configuration

Q_2.[17] The workspace defines the end effector configurations, which can be reached.[4,16] *Task space* is the space of a specific task of which the motion of the robot's end-effector obtains during this task.[4,16]

The *configuration manifold* means all the possible positions for the defined manifold of the locally Euclidean space. The *configuration manifold* (*C-manifold*) is represented by the (Q_3= SE(3) $\times S^1 \times S^1$ =*GM*) as the positioning in the SE(3) using the base manifold $S^1 \times S^1$.[16,17] Since the $S^1 \times S^1$ manifold structures the revolute rotational joints of the locally Euclidean space, the result of the *C-manifold* of Q_3 as a result within the SE(3) group is the locally Euclidean space system of another manifold. The group structure of SE(3) assigns to the *C-manifold* of the Q_3. The assignment achieves the matching the group of the displacements with the *C-space* of Q_1.[18]

While the base $S^1 \times S^1$ defines the manifold as *M*, the SE(3) defines the Lie group as *G*.[19] The shape term considers the *C-manifold* that is isomorphic to the shape of the 2-RR modular robots. Additionally, the article in this study here modified the shape space of the $S^1 \times S^1$ for the potential shape variables of the α_{1-4}, θ_1, and θ_2, having configured the modular *C-manifolds* of the skew revolute joints. The M-GLAT method can manipulate to develop algorithms of the systematic trajectories reliant on the differential geometry as defined in the literature[19] for modular *C-manifold* of 2-RR grippers. The M-GLAT algorithm, structured as a novel toolbox, is programmed in Maxima.

Manifold, a space qualification definition in topology, acts with a criterion of behaving locally in Euclidean space.[20] The topologies of the line and circle correspond to the prismatic and revolute joints in terms of motion types, respectively. The manifolds of circle S^1 or line structures the body coordinate systems, which have a property of topological space defined as locally.[20] The reduced shape variables, shape control, and shape variables are the terminology of the mechanisms for kinematics and the dynamics of manifolds in literature.[16,21] The specified shape variables of the $\theta_{1,2}$ and α_{1-4} are substituted with the constant values of the manifold's shape structure for kinematic analysis in this article. Meanwhile, the rest called the reduced shape variables changed in arranged range for workspace and trajectory analyses of the path planning.

The modular structure analysis succeeds with the results for the mechanisms of the C-ISA 1 and 2

C-manifolds for the $(S^2 \times S^2, S^1 \times S^2, S^1 \times S^1, S^2 \times S^1)$ using the shape variables of $\theta_{1-2}, \alpha_{1-4}$. The common mechanism of the micro modular *C-manifold* enables the design of the macro modular structure with a C-ISA *C-manifold* of the kinematic equations derived using the M-GLAT method. The angle in between the skew axes specifies the common mechanisms modularly for the defined *C-manifolds*.

The purpose of the C-ISA *C-manifold* of the skew revolute joints for the 2-RR modular robotic gripper with this research article is to generate novel various kinematic geometries as workspaces using the six shape variables of the $\theta_{1,2}$ and α_{1-4} for the shape spaces of $S^1 \times S^1$ and possibly S^2. Upon designing the micro modular *C-manifolds*, the angle between the skew axes for invented configurations shapes the modularity within the common mechanisms of micro modular *C-manifolds*. This angle describes the relative integration of each unique C-ISA structure for 2-RR modular robot gripper designs, as shown in Fig. 1 with θ_{1-2} and α_{1-4}. The l_1 is the length of the rigid body as link 1. Moreover, the lengths r_1 and r_2 are the centers of gravity of links 1 and 2, respectively. The twisted hand example[22] is indicating

the high versatility of the gripper designs. Macro modular *C-manifold* established with the variation in the relative poses combinations of each unique micro modular 2-RR *C-manifold* design parallelly or serially, as shown in Fig. 2. The workspaces are analyzed based on the parameters of C-ISA1, C-ISA2, θ_1, and θ_2 for micro and macro modular *C-manifold* of mechanisms, as shown in Figs 1 and 2, respectively. The micro *C-manifold* cases are relative positions of the C-ISA 1-2 for the parametric values of α_1, α_2, α_3, and α_4. Having created γ_1 between the C-ISA 1 and C-ISA 2 for the micro modular *C-manifold* as shown in Fig. 1, the combinations of γ_1 micro modular *C-manifold* with the γ_2 are the characteristic parameters of macro modular *C-manifold* as in Fig. 2.

The relative integration of the micro modular *C-manifolds* of the macro mechanism in Fig. 2a, a limb with four C-ISA of two relative angles, occurs between the micro *C-manifolds* of the γ_1 angle and γ_2 angles. The 2-RR gripper for the micro and macro modular *C-manifolds* obtain validated results of the skew revolute joint as common mechanisms via the developed analysis methodology within this article. Thus, the content of the macro modular robot grippers
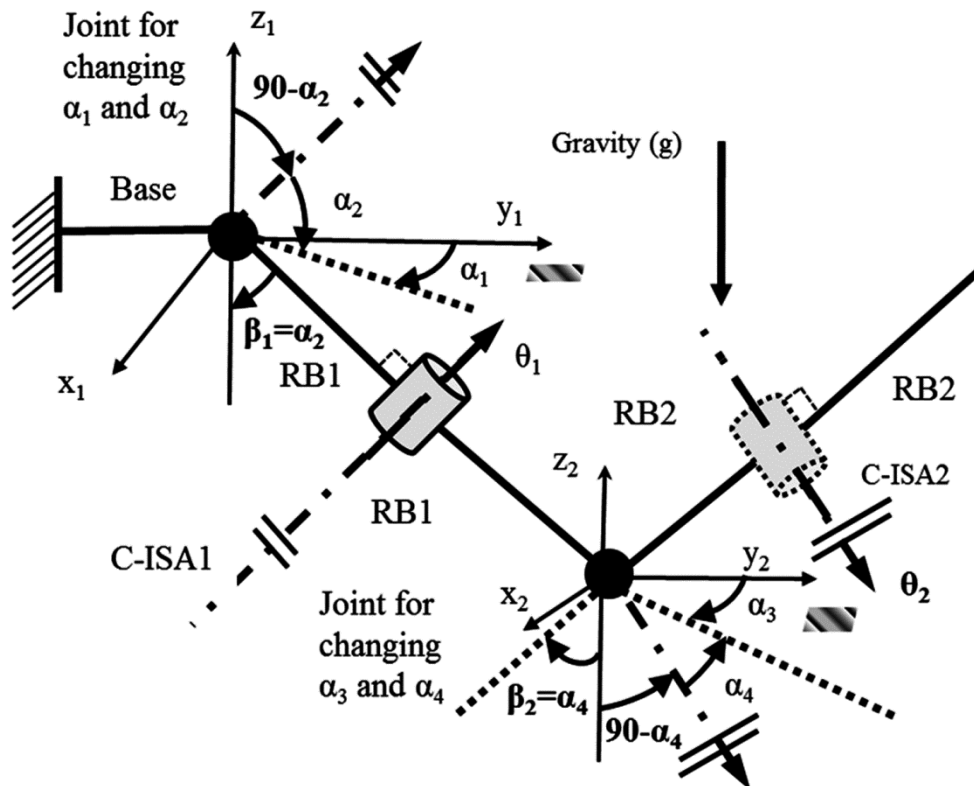

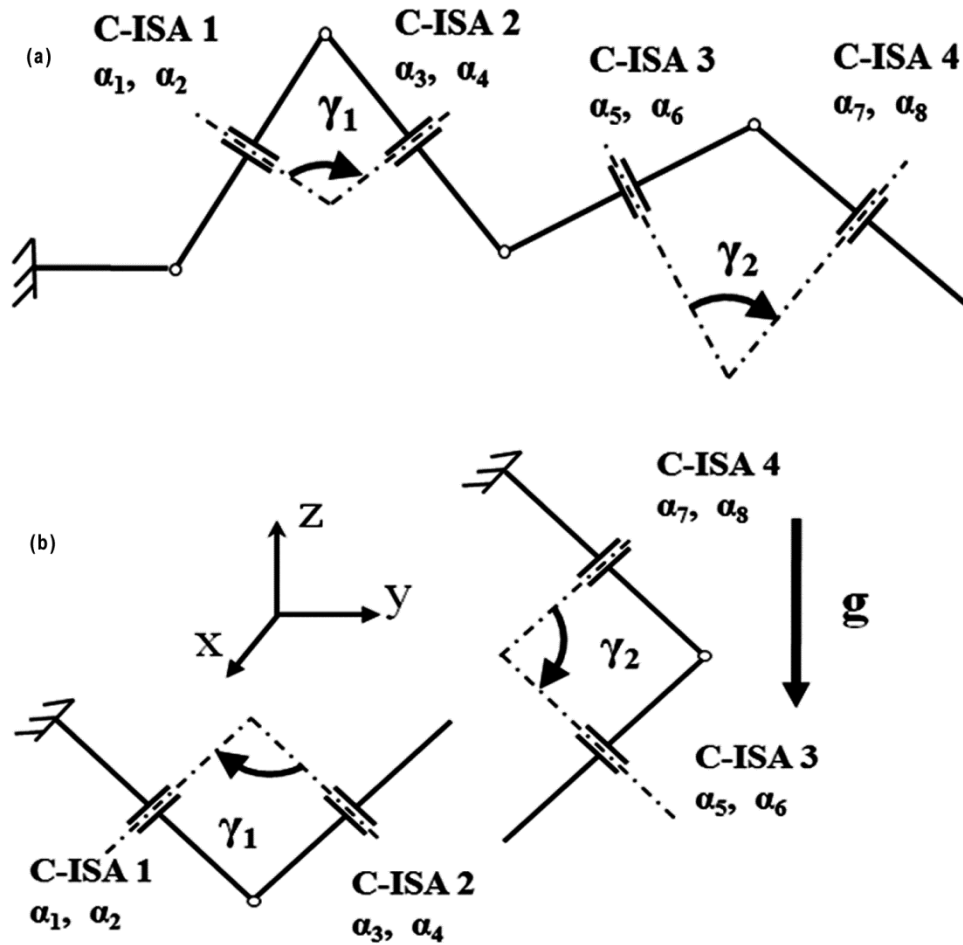Fig. 1 — Micro modular *C-manifold* design of 2-RR grippers

Fig. 2 — Macro modular C-manifold design of 2-RR serial gripper mechanisms of the γ_1, and γ_2 for robots — (a) Serial macro modular C-manifold design; (b) Parallel macro modular C-manifold design

is classified into three distinguished categories, which are serial, parallel, and hybrid modular types for 2-RR spatial mechanisms.

The α_{1-4} angles are solved for the constant angle in between C-ISA 1 and C-ISA 2. These specified angles are utilized in the derived EOMs from M-GLAT. Meanwhile, the same α_{1-4} angles are realized in the workspace equations derived from the M-GLAT. Finally, the dynamics and the workspaces are analyzed for the constant angle between C-ISA 1 and 2. The modular grippers of the robots are designed using the parallel macro modular *C-manifolds*, as shown in Fig. 3. The two vertically concentric C-ISA of the first revolute joints integrate with the two parallel C-ISA of the second revolute joints shown in Fig. 3a. The perpendicular C-ISAs of the first and second joints are constructed modularly to join, as shown in Fig. 3b.

The macro modular *C-manifold* determines the shape variables of the $\alpha_{1-8} - \theta_{1-4}$ for 4-RRRR in Fig 3. Additionally, the angles in between skew axes of the C-ISAs as γ in Fig. 2 are arranged for grasping. Besides, these grasping arrangements are designed for the workspaces determined from the results section. The novelty subject of this article is the development of the M-GLAT method for derivation of the constraint-based workspaces with the shape variables $(\alpha_{1-4} - \theta_{1,2})$ in the field of the 2-RR gripper mechanisms. Additionally, the robot dynamics of the constraint- based workspaces are developed for varied configurations of α_{1-4} with ICs of $\theta_{1,2}$. Parallel, serial, and hybrid 2-RR modular designs define the macro modular mechanism structure of which numerical results for specific cases of spatial coordinate kinematic positions of the configurations are obtained with generalized symbolic mathematics results of
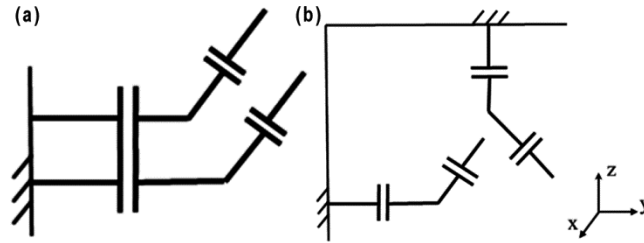
Fig. 3 — The examples of the modular 2-RR gripper designs — (a) 3-RRR: 2 ⊙ vv - 2 ‖; (b) 4-RRRR: 2 ⊥ vh - 2 ⊥

M GLAT. The same equations obtained via the M-GLAT can also be derived as in the specified references.[7]

However, the M-GLAT method for the grippers with the six shape variables can derive the modular generalized *constraint*-based workspace and dynamic equations for all cases of the *C-manifolds*. The same circumstances can be possible for the derived Equations in Appendices of the A1 and A2.[7] Besides, the 2-RR gripper mechanism is expanded for the n-R grippers with the expanded version of the M-GLAT. Therefore, the M-GLAT is used to develop workspaces with dynamics for the various kinds of grippers.The defined symbolic formulas in M-GLATare $Ad_{(g_{1j\_2})}\xi^S_{1j\_2j}$ for spatial workspace, and $Ad^{-1}_{(g_{1j\_2})}\xi^B_{1j\_2j}$ for body workspace.[4] The results of modular 2-RR gripper workspaces have many possibilities for the shape variables of $(\alpha_{1-4} - \theta_{1,2})$ using the M-GLAT method. The simplified M-GLAT results for the adjoints are in Appendix A2[7] for the skew revolute joints of the C-ISA 1 and C-ISA 2.

Methodology

The Modular C-Manifold Design of Workspaces with the Angle Between Joint 1 and Joint 2

Kinematics was analyzed using the constraints of the angle between two C-ISA. The scalar multiplication of the two C-ISA vectors occurs to solve for constraint angle in between two C-ISA for modular configuration dependent robot kinematic design, as shown in Eq. A1[7]of Appendix. The defined scalar product equation determined solving Eq. A1. Then, the specified equation defined in between 0 and π is solved according to the constraint angle between C-ISA 1 and C-ISA 2. A nonlinear numeric solver of the Newton-Raphson iteration method is used to solve it in Maxima.

Upon defining the reduced shape variables of *u* and *v* functions in terms of θ_1 being *u* and, θ_2 being the *v*, the surface plot realized using the *configuration manifold*

function of $Ad_{(g_{1j\_2})}\xi^S_{1j\_2j}$ in Maxima. As reduced shape variables, θ_1 and θ_2 parameters varied between the requested angular ranges to construct the established workspace surfaces out of the *configuration manifold* functions of the *x, y,* and *z* coordinate components of 2-RR modular grippers. The definition of the *configuration manifold* function of *u, v* can be any two parameters of shape variables to solve *x, y,* and *z* of $Ad_{(g_{1j\_2})}\xi^S_{1j\_2j}$ for workspace analysis of the 2-RR modular robots. I solved kinematic adjoints with twist equations of the C-ISA 1 and C-ISA 2 for specified constraint angle value between C-ISA 1 and C-ISA 2, as shown in Fig 4a. The 2-RR grippers design the macro modular structure with the angle γ in between C-ISA 1 and C-ISA 2. The parameter of the angle between C-ISA 1 and C-ISA 2 affects the kinematics and dynamics of the modular grippers. The $\pi/2$ radian swept around axes for θ_1, and θ_2 establishes the workspaces of the area without overlapping for some of them. In other words, the swept range increase reduces the quantity of the non-overlapping workspaces. The 23 workspace areas of G's are created from the i = 0−22, as shown in Fig. 4a. Some of the workspaces without overlapping among them are selected, as seen in Fig. 4b.

The reduced shape variables of *u* and *v* define the workspace analysis within the specified ranges. The result for the workspace is a vector space of the 6×1 on SE(3). The adjoint matrix of the 6×6 on SE(3) multiplies with the spatial twist of the 6×1 on the se(3). The result of matrix multiplication obtains the workspace of the 6×1 matrix on the SE(3). The workspace vector elements map starting from the first row as the (*x, y, z*) orthogonal axes of the chart. The results of the $f_{ox}, f_{oy},$ and f_{oz}, as seen in Eq. 1[16–19], are the *configuration manifold* functions with the total original shape variables of $\alpha_{1-4}, \theta_{1,2}$.

$$f_{ox}(\alpha_{1-4},\ \theta_{1,2}) =\ Ad_{(g_{1j\_2})}\xi^S_{1j\_2j}(1,1); f_{oy}(\alpha_{1-4},\ \theta_{1,2}) =$$
$$Ad_{(g_{1j\_2})}\xi^S_{1j\_2j}(2,1)\ ;$$

$$f_{oz}(\alpha_{1-4}, \ \theta_{1,2}) = \ Ad_{(g_{1j\_2})}\xi^S_{1j\_2j}(3,1) \qquad \ldots (1)$$

Upon substitution of the constant values for the α_{1-4} in the shape variables, the *C-manifold* of the functions is generating workspaces using the reduced shape variables projected on the *xyz* axes as in Eq. 2.[16–19,23]

$$f_{rx}(u,v) = f_{ox}(\alpha_{1-4}, \theta_{1,2}) = x(\theta_1, \theta_2) \,, \ u = \theta_1, v = \theta_2 \ ; \ f_{ry}(u,v)$$
$$= f_{oy}(\alpha_{1-4}, \theta_{1,2}) = y(\theta_1, \theta_2) \,, \ u = \theta_1, v = \theta_2;$$
$$f_{rz}(u,v) = f_{oz}(\alpha_{1-4}, \theta_{1,2}) = z(\theta_1, \theta_2) \,, \quad u = \theta_1, v = \theta_2 \ \ldots (2)$$
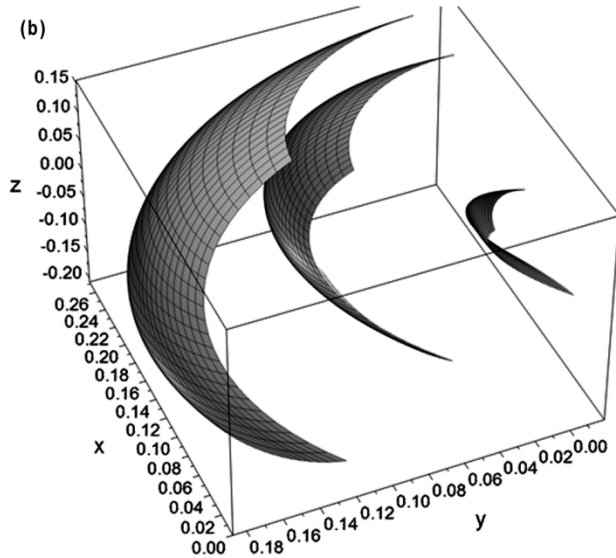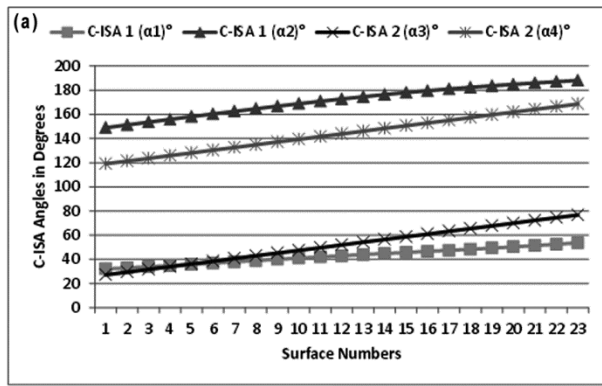

Fig. 4 — The solution of the α_{1-4} for the constant $\pi/6$ angles in between C-ISA 1 and 2, x, y and z (in meters) — (a) G1-23 sequential increments of $\pi/80$ for α_3 and α_4; (b) Non-overlapping workspaces of the G1, G10, G22

The *C-manifold* for the reduced shape variables becomes as in Eq. 3. The ranges for the reduced shape variables define the characteristics of the *C-manifold* in Eq. 3.[16–19]

$$S^1 x S^1 = \{(x, y, z) \in R^3 \colon x = f_{rx}(u,v) \,, \ y = f_{ry}(u,v), \ z = f_{rz}(u,v) \colon 0 \le u \le \tfrac{\pi}{2} \,, \ 0 \le v \le \tfrac{\pi}{2} \}, \text{ and } M_1 = \{(\theta_1, \theta_2)| \ \theta_1 \in S^1, \ \theta_2 \in S^1\} \qquad \ldots (3)$$

The Validation and Verifications of the Developed M-GLAT Method

Upon substitution of the $\alpha_{1,2,3,4} = \pi/2$, the M-GLAT method obtains the EOMs of this known case.[24–26] Then, these known equations from the literature verified the derived equations of motions from M-GLAT. Additionally, the kinematics equations of workspaces obtained from M-GLAT are verified using trigonometry of the determined geometry for the *C-manifold* of the $\alpha_{1,2,3,4} = \pi/2$. Finally, the derived adjoints and the inverse adjoints via M-GLAT are validated and verified with the results already available in various references for specific simple configurations of the 2-RR robots.[3,4,20]

The Robot Dynamics of Skew Revolute Joints for Varied Configurations of α_{1-4} with ICs of θ_{1-2}

The symbolic mathematics with Lie algebra toolbox M-GLAT was developed to derive EOMs. Thus, the algorithm of the Maxima is developed using the kinematics of the Lie algebra and the Lagrange method for derivation of the EOMs. The parameter values for dynamics are in Table 1.

The derived EOMs have the six shape variables of the θ_{1-2} and α_{1-4} for skew revolute joints. Gripper dynamics are defined for skew revolute considering the varied configurations of α_{1-4} with ICs of θ_{1-2}. The dynamics for $\alpha_{1-4} = \frac{\pi}{2}$ are the known EOMs[24] derived from the generalized EOMs using M-GLAT. The nonlinear numerical analysis method is described via the solvable first-order ODEs. Thus, the nonlinear state-space of the EOMs structured exactly to solve in the Maxima. Appendix A3 is describing the fundamental structure of the EOMs derived via M-GLAT. Having applied these generalized fundamental EOMs according to the references[2–4], the EOMs obtained with the defined six shape variables via M-GLAT. The generalized EOMs using the

Table 1 — Modular 2-RR gripper of the robot parameters					
l_1	0.2 m	I_{z1}	0.2 kgm^2	I_{y2}	0.2 kgm^2
r_1	0.1 m	I_{x2}	0.2 kgm^2	I_{z2}	0.2 kgm^2
r_2	0.1 m	m_1	1 kg	m_2	1 kg

C-ISA *configuration manifolds* are validated and verified with the known EOMs derived. The verification of the M-GLAT is made possible by the known EOMs for specific cases.[24–26]

Results

Results for Task Space Algorithm with the Angle Between C-ISA 1 and C-ISA 2

Upon defining the constant $\pi/6$ angle in between C-ISA of *C-manifolds*, the increment of $\pi/20$ confined the α_3 and α_4. The angle between the C-ISA of *C-manifolds* is determined using the shape variables of the α_{1-4} in the methodology section. The spatial trajectory planning occurs for γ angle in between C-ISA 1 and C-ISA 2. Thus, the workspace algorithms create trajectory planning via the angle parameter between C-ISA 1 and C-ISA 2. The modular micro and macro *C-manifold* designs obtained the workspace algorithms of the 2-RR gripper, which is expandable into the higher modular revolute joints of the n-R for the grippers. The n-R modular expandable grippers are increasing the precision and power grasping capability. Having contained the constant angle of $\gamma = \pi/6$ in between C-ISAs, the α_3 and α_4 analyzed for the 23 consecutive increments of $\pi/20$, $\pi/40$, and $\pi/80$. The characteristic shape of the workspaces is similar for the α_3 and α_4 of $\pi/20$ and $\pi/40$ intervals. The non-overlapping workspace plot for $\pi/80$ increment is in Fig. 4.

The specified γ angle in between C-ISA 1 and 2 in this article is a characteristic parameter identified for modular grippers. The consequence of this research article is the spatial *C-manifold* via mechanism-based designs of the C-ISAs for a 2-RR and n-R modular gripperof novel workspaces with dynamics results. Additionally, the $\theta_{1,2}$ angles are swept in a range of 0 to $\pi/2$ radians to construct the workspaces for all cases with varied workspaces result of C-manifolds. When the angle $\pi/6$ is constant in between the two C-ISAs, the equations are solved for the 23 consecutive increments for α_3 and α_4 listed in Fig. 4. The non-overlapping plots are selected from Fig. 4b with the x, y, and z axes in meters. Upon defining the constraint angle of $\gamma = \pi/6$ in between C-ISAs, the algorithm with the α_3 and α_4 solved the increments of $\pi/80$. The nonlinear numerical algorithm of the Newton-Raphson method is used in Eq. A1 to solve for α_{1-4} with the 23 consecutive increments of $\pi/80$.

The result of the developed algorithm defines the C-ISA 1 and 2 formulations of the shape variables α_{1-4} derived from the scalar product, as shown in Eq. A1 in

the appendix. The compact with various sizes achieves to structure the workspaces for the macro modular *C-manifolds* in Fig 4b. The workspaces for these 2-RR modular grippers can be structured to work synchronously. The design procedure of the workspaces for the 2-RR modular grippers generates the results in Fig 4b using the kinematic equation of the $Ad_{(g_{1j\_2})}\xi^S_{1j\_2j}$. These workspaces are designed not to have overlapping regions, the requirement for collision avoidance, within multi-robot and multi-finger gripper applications. Besides, the workspaces are designed to work concurrently and synchronously. The result of adjoints in Appendix A2 is limited for specific *C-manifold* due to limited space in this article.

The multiple workspaces without overlapping were created with the minimum angle increment of $\pi/80$ between the C-ISA 1 and 2. I observed reducing the increment of the angle for multiple workspaces was changing the characteristic area of the workspace designs of the 2-RR gripper. This spatial workspace analysis using the M-GLAT method is successful in creating workspaces with varied characteristics for the grasping of the grippers. There are sequential non-overlapping workspaces of the G2-G10 and G16-G21 with the increments of $\pi/20$ for the α_3 and α_4. Additionally, there are many possibilities to select the non-overlapping workspaces from the G0-G22 workspaces. There are sequential non-overlapping workspaces created of the G4-G22 with an increment of $\pi/80$ for the α_3 and α_4. Additionally, there are sequential non-overlapping workspaces created of the G2-G22 with an increment of $\pi/40$ for the α_3 and α_4. The constant angle in between the C-ISA 1 and 2 is generating similar shapes of the workspaces for the cases of ($\pi/20$, $\pi/40$, $\pi/80$). The created *C-manifolds* of constraint angle between C-ISA 1 and C-ISA 2 are defined for the *task space* algorithms of the 2-RR modular grippers. The maximum C-ISA angle reached for the 23rd surface is the least for $\pi/80$ of Fig.4a compared to the $\pi/20$ and $\pi/40$. The collision avoidance of the fingers for the grippers can be realized with the analysis results here. One can select a combination of C-manifolds of ($\pi/20$, $\pi/40$, $\pi/80$) for the workspace requirements of the gripper finger designs as the grasp surfaces to control.

Results for the Modular Spatial Gripper Dynamics for Varied Configurations of α_{1-4} with ICs

The comprehensive phase plane plotted for the angular velocity (rad/s) versus angular position (radian) in Fig. 5 for various shape variables α_{1-4} and
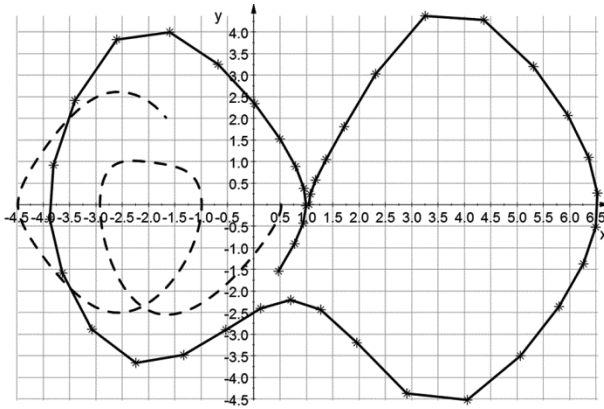
Fig. 5 — x and y axes are θ_2 (rd) and $\dot{\theta}_2$(rd/sec) respectively for C-manifold of (α_{1-4}= π/6, π/3, π/6, π/3)

ICs of the $\theta_{1,2}$ angles with the C-ISA configuration manifolds. While the kinematics equations structure the constraint-based design of the workspaces, the dynamics with the derived EOMs apply to the skew revolute joints for developing the grasp planning of the grippers. The dynamics of the EOMs with workspaces are needed for realizing the grasp planning.

The motion strategies for various initial conditions of $\theta_{1,2}$ angles are analyzed based on the *C-manifold* of the C-ISA with shape variables of the α_{1-4}. M-GLAT is capable of deriving the constraint based workspaces with dynamics of the EOMs. Responses based on the various skew axes of α_{1-4} for the ICs of the $\theta_{1,2}$ construct the velocity versus position requirements for the actuator design of the modular 2-RR grippers in the skew revolute joints. The quantity of sine and cosine terms of the EOMs are decreasing when the shape variables of the α_{1-4} are ($\forall\, \alpha_{1-4} \in R \ for\ i \in \mathbb{Z}, \quad \alpha_{1-4} = i\frac{\pi}{2}$).[17] The cosine and sine terms of the $i\pi/2$ are zero or 1 with orthogonal or parallel axes. Therefore, the results of the EOMs are simplified when the two of the α_{1-4} are $i\pi/2$ for the integer i values. The geometry transforms into the horizontal orientation with parallel non-skew axes when the α_{1-4} angles are equal to the π/2 for skew revolute joints. The results for the created configurations are shown in Fig. 5 of the (α_{1-4}= π/6, π/3, π/6, π/3) respectively for the ICs of the $\theta_{1,2}$ angles. The legends of the lines in the plots for ICs have dashed line represents the (θ_2= π/6, θ_1=0), and solid line with star point represents the (θ_2= π/3, θ_1=0). The simulated time for EOMs is 40 seconds. The ICs for the phase plots of the θ_2 and $\dot{\theta}_2$ are (θ_2= π/3, π/6) and (θ_1= 0, 0) for C-manifold of (α_{1-4}= π/6, π/3, π/6, π/3) in Fig. 5.

The phase plots are the solutions of the derived EOMs via the M-GLAT method for the substituted values of the α_{1-4}. The results of the α_{1-4} = π/2 for the position and velocity plots are zero since this scenario is a complete horizontal configuration for both the first and second links. The dynamics of the double pendulum problem in the literature is the most widespread application in controls. Therefore, it is fundamental to obtain the constraint-based most comprehensive dynamics and kinematics equations that have the most applicability in the multibody dynamics control problems.

Discussion

The M-GLAT of the micro and macro gripper mechanism is derived and analyzed workspaces with dynamics for the specified constant angle between C-ISA 1 and C-ISA 2. The developed rule-based and constraint-angle dependent workspace analyses can serve to progress in the field of the algorithm for task-space based motions, which are reliant on the modular *C-manifold* design with shape variables of the ($\alpha_{1-4}-\theta_{1,2}$). Additionally, the novel dynamics equations determine these task-space dependent algorithm development with novel EOMs based on the same shape variables of the ($\alpha_{1-4} - \theta_{1,2}$). The qualifications of the advanced robotic grasp technologies rely on the requirement of the surface trajectory tracking control via the 6-DOF closed-loop design[27] Since the problem of path planning for multiple robots requires an accurate model of the workspaces[28], this article contributes to establishing accurate workspaces of 2-RR and expandable n-R grippers for path planning and grasping. The cost-effective modularity with path planning[29] is feasible using the state-of-the-art technologies of soft robotics[30] and mobile household robots.[31]

The skew axes of n-R grippers with specified dynamics and constraint based workspace equations, as derived with this article here, have potential progress in the design of the multi-fingered robotic hands.[10] The complete constraint- based parametric workspaces with dynamics analyses of the serial mechanisms are not available for the grippers with skew revolute. Thus, the research in constraint of angle in between C-ISA based workspace with dynamic completed of this article can lead the design of the skew axis related hands and wrist mechanisms with functional designs using the M-GLAT developed herein. The nonlinear EOMs are solved numerically

using the Runge-Kutta (RK) method in Maxima. All the EOMs for various *C-manifolds* of α_{1-4} can be generated using the general EOMs with specified values of the α_{1-4}. Then, the differential equations of the substituted α_{1-4} angles are solved for the ICs of the $\theta_{1,2}$ using the RK. The phase plots of the simplified EOMs derived using M-GLAT are validated and verified by the known EOMs for 2-RR robots. These known EOMs are derived and available as the double pendulum problems in the literature.[24–26]

Upon determining the *task space* and *workspace* for 2-RR modular grippers, the details of the configuration dependent modular design can further progress via specifying the *C-manifolds*. While the C-ISA 1 manifold has the shape variables of the θ_1 and $\alpha_{1,2}$, the C-ISA 2 has the shape variables of θ_2 with $\alpha_{3,4}$. After selecting the shape space for *C-manifold* as $S^1 \times S^1$ or $S^2 \times S^2$, the 2-RR modular robot design constructs the requirements of the task spaces for the robotic systems considering the shape variables. Learning algorithm manifolds for dexterous fingers of skew revolute joints can be defined for the grasp planner utilizing the kinematic and dynamic equations developed as *C-manifolds* with the article here. The created *sequential non-overlapping workspaces*, in the results section herein, are convenient in grasping the homogeneous symmetrical shapes stably with multiple fingers.

Conclusions

The micro and macro 2-RR modular grippers were investigated and designed via configuration dependent modular designs of C-ISA in this article. These configuration dependent modular components were analyzed in the previous sections as the C-ISA angles, which are modified for the configuration of the 2-RR modular grippers using the manifold of the Euclidean space in body coordinate. The fingers without collision for the grippers were designed based on the non-overlapping workspaces developed here. The constraint angle design in between axes of the skew revolute joints provides the contained specific grasp capability of the gripper. This design approach produces dexterity with the modular grasp workspaces for the gripper fingers with skew revolute joints. The constraint based workspaces with dynamics of the EOMs herein are the value added analyses capability of the developed M-GLAT for the spatial micro and macro modular gripper mechanisms.

The developed method of M-GLAT conveys the mapping from the Lie group SE(3) to the Lie algebra se(3) through the subjects of the differential geometry. The specified constraint based analyses of the 2-RR modular gripper workspaces with dynamics of equations for skew revolute joint are revealed. The novel workspaces were created for multiple modular 2-RR grippers with and without overlappings. The modular grippers have common mechanisms that can be modified as a modular configuration-based design approach for increasing the functionality using the abstract mathematics of the differential geometry. These common mechanisms of the modular robots can be structured using the manifolds of varied shapes for the required configurations. The mechanism configurations of the shape variables $\theta_{1,2}, \alpha_{1-4}$ were changed dynamically for 2-RR modular robots via the angle in between the C-ISA 1 and C-ISA -2.

The 2-RR modular grippers of the common mechanisms are tested via the micro and macro *C-manifolds* of the kinematic equations derived from the M-GLAT method. The algorithm results unveil the diversification of the created workspaces through the α_{1-4} shape variables of the C-ISA 1 and 2. The high potential of the structured workspaces handles to manipulate the 2-RR modular grippers in widespread automation applications. Modular configuration manifolds of the shape variables $(\alpha_{1-4} - \theta_{1,2})$ were created of the skew revolute joints for 2-RR through the dynamics and kinematics equations. Many applications with coherent results further progressed with the modularity and versatility of the serial grippers. The systematic workspace methods developed were applied with the M-GLAT method for modular *C-manifold* of 2-RR and expandable n-R grippers. The algorithms of task spaces have relied on the novel workspaces developed with this article. Finally, the designed novel dexterous multi-grippers of the modular 2-RR and n-R *C-manifolds* can program the task spaces precisely by applying these algorithms. Furthermore, this modularity is crucial for the mechatronic systems integrated into sensory-robotics applications.

References

1 Zeghloul S, Laribi M A & Arevalo J S S, *Advances in Service and İndustrial Robotics* (Springer) 2020, 1–609.

2   Müller A, Screw and Lie group theory in multibody dynamics recursive algorithms and equations of motion of tree-topology systems, *Multibody Syst Dyn*, **42** (2018) 219–248.

3   Müller A, Screw and Lie group theory in multibody kinematics motion representation and recursive kinematics of tree-topology systems, *Multibody Syst Dyn*, **43** (2018) 37–70.

4   Murray R M, Li Z & Sastry S S, *A Mathematical İntroduction to Robotic Manipulation*, (CRC Press)1994, 1–474.

5   Wei J & Dai J S, Lie group based type synthesis using transformation configuration space for reconfigurable parallel mechanisms with bifurcation between spherical motion and planar motion, *ASME J Mech Des*, **142(6)** (2020) 1–13. https://doi.org/10.1115/1.4045042.

6   Müller A, An overview of formulae for the higher-order kinematics of lower-pair chains with applications in robotics and mechanism theory, *Mech Mach Theory*, **142** (2019) 1–35.

7   Reiter A, *Optimal Path and Trajectory Planning for Serial Robots* (Springer) 2020, 1–201. https://doi.org/10.1007/978-3-658-28594-4.

8   Ayalon Y, Damti L & Zarrouk D, Design and modelling of a minimally actuated serial robot, *IEEE Robot Autom Lett*, **5(3)** (2020) 4899 –4906. https://doi.org/10.1109/LRA.2020.3004783.

9   Nichols J A, Bednar M S, Havey R M & Murray W M, Decoupling the wrist: A cadaveric experiment examining wrist kinematics following midcarpal fusion and scaphoid excision, *J Appl Biomech*, **33(1)** (2017) 12–23. https://doi.org/10.1123/jab.2015-0324.

10   Deemyad T, Hassanzadeh N & Perez-Gracia A, Coupling mechanisms for multi-fingered robotic hands with skew axes, 344–352 (2019). in *Mechanism Design for Robotics*, edited by Gasparetto A & Ceccarelli M, MEDER 2018, Mechanisms and Machine Science, vol 66, (Springer Cham) https://doi.org/10.1007/978-3-030-00365-4_41.

11   Sommer III H J & Miller N R, A technique for kinematic modeling of anatomical joints, *ASME J Biomech Eng*, **102(4)** (1980) 311–317, https://doi.org/10.1115/1.3138228.

12   Thiruvengadam S & Miller K A, Geometric algebra based higher dimensional approximation method for statics and kinematics of robotic manipulators, *Adv Appl Clifford Algebras*, **30(17)** (2020) 1–43, https://doi.org/10.1007/s00006-019-1039-z.

13   Peng S, Yan Biao L, Ze Sheng W, Ke C, Bo C, Xi Z, Jun Z & Yi Y, Inverse displacement analysis of a novel hybrid humanoid robotic arm, *Mech Mach Theory*, **147** (2020) 1–21. DOI:10.1016/j.mechmachtheory.2019.103743.

14   Figliolini G, Rea P & Angeles J, The Synthesis of the axodes of RCCC linkages, *J Mech Robot*, **8** (2016) 1–9.

15   Flores P, Modeling and simulation of wear in revolute clearance joints in multibody systems, *Mech Mach Theory*, **44(6)** (2009) 1211–1222.

16   Silvia E & Harald S, Applying differential geometry to kinematic modeling in mobile robotics, 2005 *WSEAS Int Conf Dynam Syst Control*, (Venice, Italy) November 2–4, 2005, 106–112.

17   Novelia A & O'Reilly O M, On the dynamics of the eye: Geodesics on a configuration manifold, motions of the gaze direction and Helmholtz's Theorem, *Nonlinear Dyn*, **80** (2015) 1303–1327, https://doi.org/10.1007/s11071-015-1945-0.

18   Travers M, Whitman J & Choset H, Shape-based coordination in locomotion control, *Int J Robot Res*, **37(10)** (2018) 1253–1268. https://doi.org/10.1177/0278364918761569.

19   Watterson M, Liu S, Sun K, Smith T & Kumar V, Trajectory optimization on manifolds with applications to quadrotor systems, *Int J Robot Res*, **39(2–3)** (2020) 303–320, https://doi.org/10.1177/0278364919891775.

20   From P J, Jan Tommy Gravdahl & Pettersen K Y, *Vehicle-Manipulator Systems Modeling for Simulation, Analysis, and Control* (Springer) 2014, 1–388.

21   Giovanni S L, Michael S, Dimitris T P, Arianna M & Paolo D, Polychaete-like undulatory robotic locomotion in unstructured substrates, *IEEE Trans Robot*, **23(6)** (2007) 1200–1212. https://doi.org/10.1109/TRO.2007.909791.

22   Lee K, Wang Y & Zheng C, TWISTER Hand: Underactuated robotic gripper ınspired by origami twisted tower, *IEEE Trans Robot*, **36(2)** (2020) 488–500, DOI: 10.1109/TRO.2019.2956870.

23   Belta C & Kumar V, Abstraction and control for groups of robots, *IEEE Trans Robot*, **20(5)** (2004) 865–875, https://doi.org/10.1109/TRO.2004.829498.

24   Awrejcewicz J & Sendkowski D, Geometric analysis of the dynamics of a double pendulum, *J Mech Mater Struct*, **2(8)** (2007) 1421–1430, https://doi.org/10.2140/jomms.2007.2.1421.

25   Rafat M Z & Wheatland M S & Bedding T R, Dynamics of a double pendulum with distributed mass, *Am J Phys*, **77(216)** (2009) 216–223, https://doi.org/10.1119/1.3052072.

26   Sun N, Wu Y, Chen H & Fang Y, An energy-optimal solution for transportation control of cranes with double pendulum dynamics: Design and experiments, *Mech Syst Signal Process*, **102** (2018) 87–101. https://doi.org/10.1016/j.ymssp.2017.09.027.

27   Song S, Zeng A, Lee J & Funkhouser T, Grasping in the wild: Learning 6DoF closed-loop grasping from low-cost demonstrations, *IEEE Robot Autom Lett*, **5(3)** July 2020, https://doi.org/10.1109/LRA.2020.3004787.

28   Gómez-Bravo F, Carbone G & Fortes J C, Collision free trajectory planning for hybrid manipulators, *Mechatronics*, **22(6)** (2012) 836–851. https://doi.org/10.1016/j.mechatronics.2012.05.001.

29   Kalpitha N & Murali S, Optimal path planning using rrt for dynamic obstacles, *J Sci Ind Res*, **79** (2020) 513–516.

30   Dilibal S, Sahin H, Danquah O, Emon M O F & Choi J W, Additively manufactured custom soft gripper with embedded soft force sensors for an ındustrial robot, *Int J Precis Eng Manuf*, **22** (2021) 709–718, https://doi.org/10.1007/s12541-021-00479-0.

31   Sahin H & Guvenc L, Household robotics: autonomous devices for vacuuming and lawn mowing, *IEEE Control Syst Mag*, **27(2)** (2007) 20–96, doi: 10.1109/MCS.2007.338262.

Appendix

A1) The complete EOMS and adjoint matrices obtained from M-GLAT are not included in this article, due to complexity of the equations. The equation of the scalar multiplication of the angle between the C-ISA 1 and C-ISA 2 is in the following equation. The generalized equations between two ISA's are already derived using the scalar multiplication from references.[7]

$$cos^{-1}\left(\frac{(sin(\alpha_4)\,sin(\alpha_2) + cos(\alpha_3)\,cos(\alpha_4)\,cos(\alpha_1)\,cos(\alpha_2) + cos(\alpha_4)\,sin(\alpha_3)\,cos(\alpha_2)\,sin(\alpha_1))}{\begin{array}{c}(sin(\alpha_2)\,sin(\alpha_2) + cos(\alpha_1)\,cos(\alpha_2)\,cos(\alpha_1)\,cos(\alpha_2) + cos(\alpha_2)\,sin(\alpha_1)\,cos(\alpha_2)\,sin(\alpha_1)).\\ (sin(\alpha_4)\,sin(\alpha_4) + cos(\alpha_3)\,cos(\alpha_4)\,cos(\alpha_3)\,cos(\alpha_4) + cos(\alpha_4)\,sin(\alpha_3)\,cos(\alpha_4)\,sin(\alpha_3))\end{array}} \right)$$

A2) Adjoint of the transformation matrix between the first joint and the COG of the second link derived using M-GLAT: The modular C-manifold for the special case of $\alpha_1 = \frac{\pi}{2},\ \alpha_2 = \frac{\pi}{2},\ \alpha_3 = \frac{\pi}{2}, \alpha_4 = \frac{\pi}{2}$ is revealed as below.

The same equations are derived using the various methods in the literature.[7] However, M-GLAT can derive all equations for the C-manifold of the α_{1-4} and θ_{1-2} shape variables.

$\text{Ad}_{(g_{1j\_2})} =$

σ_1	σ_4	0	0	0	$-\sigma_3 - cos(\theta_2)\,\sigma_6$
σ_2	σ_1	0	0	0	σ_5
0	0	1	$\sigma_1(\sigma_3 + cos(\theta_1)\,\sigma_6 - \sigma_2\sigma_5$	$-\sigma_2(\sigma_3 + cos(\theta_1)\,\sigma_6 - \sigma_1\sigma_5$	0
0	0	0	σ_1	σ_4	0
0	0	0	σ_2	σ_1	0
0	0	0	0	0	1

where,

$\sigma_1 = cos(\theta_1)cos(\theta_2) - (sin(\theta_1)\,sin(\theta_2)),$ $\sigma_2 = cos(\theta_1)sin(\theta_2) + (cos(\theta_2)\,sin(\theta_1)),$

$\sigma_3 = sin(\theta_1)\big(sin(\theta_2)(l_1 + r_2) - l_1sin(\theta_2)\big)$, $\sigma_4 = -cos(\theta_1)sin(\theta_2) - cos(\theta_2)sin(\theta_1),$

$\sigma_5 = cos(\theta_1)\big(sin(\theta_2)(l_1 + r_2) - l_1sin(\theta_2)\big) - sin(\theta_1)\sigma_6,$ $\sigma_6 = l_1(cos(\theta_2) - 1) - cos(\theta_2)(l_1 + r_2)$

A3) Derived parametric EOMs by M-GLAT method for C-manifolds: The generalized equations used in the algorithm of the M-GLAT are from the various references[2-4]: The M_{11}, M_{12}, C_{11}, C_{12}, N_1, M_{21}, M_2, C_{22} and N_2 terms are derived symbolically for the equations of motions below via M-GLAT

EOM for the first rigid body link: $M_{11}(\theta_{1,2}, \alpha_{1-4})\ddot{\theta}_1 + M_{12}(\theta_{1,2}, \alpha_{1-4})\ddot{\theta}_2 + C_{11}(\dot{\theta}_{1,2}, \theta_{1,2}, \alpha_{1-4})\dot{\theta}_1\dot{\theta}_2 +$

$C_{12}(\dot{\theta}_{1,2}, \theta_{1,2}, \alpha_{1-4})\dot{\theta}_2^2 + N_1(\dot{\theta}_{1,2}, \theta_{1,2}, \alpha_{1-4}) = 0$

EOM for the second rigid body link: $M_{21}(\theta_{1,2}, \alpha_{1-4})\ddot{\theta}_1 + M_{22}(\theta_{1,2}, \alpha_{1-4})\ddot{\theta}_2 + C_{22}(\dot{\theta}_{1,2}, \theta_{1,2}, \alpha_{1-4})\dot{\theta}_1^2 +$

$N_2(\dot{\theta}_{1,2}, \theta_{1,2}, \alpha_{1-4}) = 0$